Always finding faults: New Zealand 2016

Kevin W. Hall[1], Helen Isaac[1], Malcolm Bertram[1], Kevin Bertram[1], Don Lawton[1], Alexis Constantinou[2], Doug Schmitt[3], Randy Kofman[3], Jennifer Eccles[4], Vera Lay[5], Stefan Buske[5], John Townend[6] , Martha Savage[6], Andrew Gorman[7] and Richard Kellett[8]

ABSTRACT

CREWES participated in two collaborative seismic programs that were conducted on the North and South Islands of New Zealand in early 2016. The South Island survey was conducted in the Whataroa Valley, primarily on unconsolidated glacial and river sediments, and consisted of a variety of vertical seismic profile (VSP) surveys in the DFDP-2b borehole, as well as surface 1C-2D, 1C-3D and 3C-3D surveys. The purpose of this survey was to better understand the Alpine Fault, which runs along the west coast of the South Island and has potential to produce M8+ earthquakes.

The North Island survey was conducted along the top of a stop-bank over unconsolidated river and marine sediments in the Hauraki Rift, and consisted of a single 1C-2D crooked-line. One of the goals of this project was to test the viability of seismic reflection surveying to image faults using a Vibe in this area. This seismic line crosses the northern Kerepehi fault, which has previously been inferred from gravity data. The Kerepehi fault is considered to be active, and is thought to have produced M6+ earthquakes in the past.

This report shows an initial comparison of fiber-optic (DAS) and geophone results for a zero-offset VSP in DFDP-2b. We also present crooked-line (1C-2D) processing results, including stacked and migrated time and depth sections across both the Alpine fault and the Kerepehi fault.

[1] CREWES, University of Calgary, Calgary, Alberta, Canada
[2] Schlumberger Fiber Optics Technology Center, Romsey, England
[3] University of Alberta, Edmonton, Alberta, Canada
[4] University of Auckland, Auckland, New Zealand
[5] Technical University Bergakadamie Freiberg (TUBAF), Freiberg, Germany
[6] Victoria University of Wellington, Wellington, New Zealand
[7] University of Otago, Dunedin, New Zealand
[8] GNS Science, Lower Hutt, New Zealand

INTRODUCTION

Two collaborative seismic programs were conducted on the North and South Islands of New Zealand in early 2016. The South Island survey was conducted in the Whataroa Valley, primarily on unconsolidated glacial and river sediments, and consisted of a variety of vertical seismic profile (VSP) surveys and surface 1C-2D, 1C-3D and 3C-3D surveys. The North Island survey was conducted along the top of a stop-bank over unconsolidated river and marine sediments in the Hauraki Rift, and consisted of a single 1C-2D crooked-line.

CREWES provided and operated the University of Calgary's IVI EnviroVibe and Inova (ARAM) Aries 600 channel seismic system. We were fairly certain this source would have a good chance of success given our experience working on surface clays and gravels in southern Alberta, and our previous work imaging faults below beach sand and sediments in the Christchurch area (Hall et al., 2011, Lawton et al., 2011, 2012, 2013; Figure 1). The University of Otago provided a 250 kg accelerated weight-drop source in case the Vibe broke down, and to orientate 3C geophones in the borehole.

The benefits to CREWES for participating in this work include (a) cost-sharing of staff with the ability to show results to CREWES sponsors; (b) imaging active fault systems, potentially beneficial for hydraulic fracturing operations; and (c) the opportunity to record and compare VSP data on co-located optical fibre and geophones.

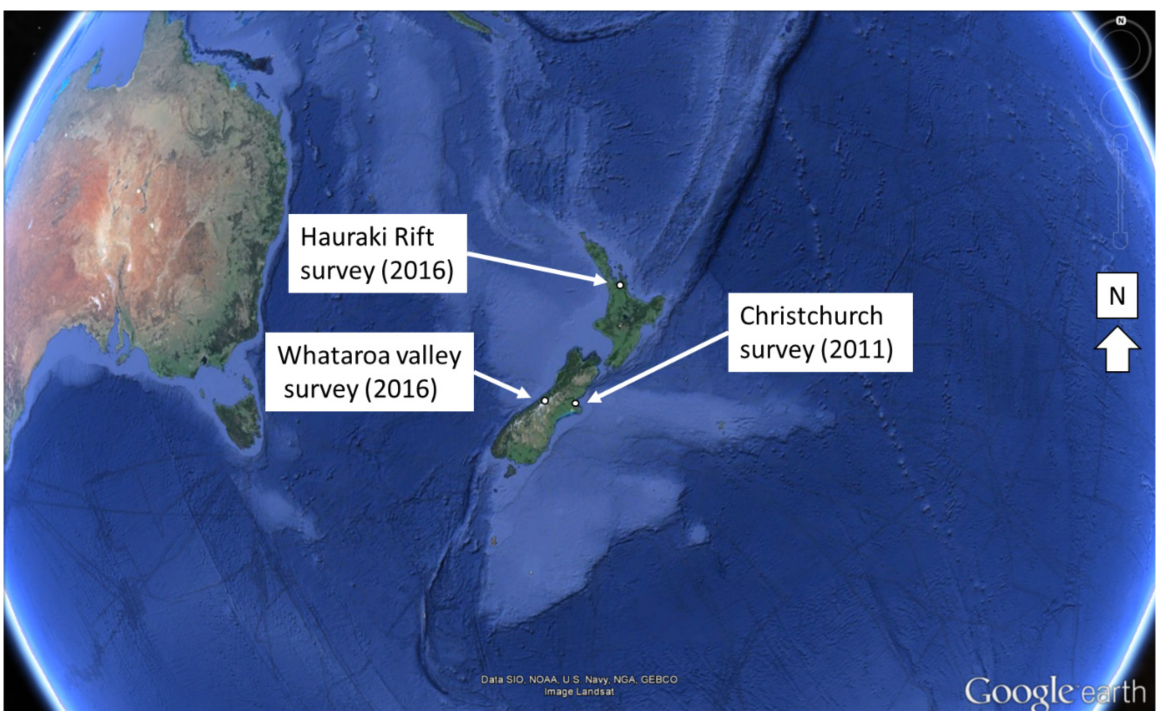

Figure 1. Location of New Zealand seismic surveys CREWES has participated in (Google Earth, 2016). Data: SIO, NOAA, U.S. Navy, NGA, GEBCO. Image: Landsat.

WHATAROA VALLEY (DFDP-2B, ALPINE FAULT)

Geology overview

The South Island survey was located in the Whataroa valley, where the target of interest is the Alpine Fault. The Alpine Fault forms part of the boundary between the Australian and Pacific Plates in southern New Zealand. It delineates the steep western front of the Southern Alps over a distance of approximately 500 km. Slip on the fault is responsible for lifting up the Southern Alps and for offsetting rocks laterally by hundreds of kilometres. During the last two million years, the central portion of the Alpine Fault has slipped at an average rate of approximately 27 mm/yr horizontally and 10 mm/yr vertically. In the Whataroa Valley the surface trace is near the range front of the Southern Alps and the Alpine Fault dips ~45˚ to the SE beneath the mountains (GNS Science Public Wiki, 2016).

DFDP-2b Borehole

The Deep Fault Drilling Project (DFDP) aims to determine the ambient conditions in a continental fault zone late in its typical cycle of large (M~8) earthquakes. A borehole (DFDP-2b) was drilled with intent to intersect the Alpine fault (Sutherland et al., 2015). The borehole is near-vertical at the surface but deviates to become normal to the fault-plane. The borehole did not intersect the fault-plane due to technical issues, but did encounter anomalously high temperatures at the bottom of the borehole. Due to a casing failure, the bottom of the borehole is filled with cement. However, the top half of the borehole remains open and can be logged. A six-strand fiber-optic cable was cemented into the borehole from surface to total-depth (TD). The drillers encountered approximately 240 m of gravels, silts and diamictites before encountering a metamorphic sequence of schist, proto-mylonite and mylonite.

Purpose of seismic work

Previous seismic surveys are summarized by Townend et al., 2016). In general, they were able to provide deep (>1 km) and shallow (<500 m) information, but it has proved difficult to image the Alpine Fault in the target 500-1000 m depth range due to energy scattered from the steep valley sides. In addition to better imaging the Alpine Fault, one of the goals of the 2016 seismic program was to conduct VSP and passive seismic surveys in the borehole using a distributed acoustic sensing (DAS) system connected to the fiber-optic cable before the fiber degraded in the hot borehole. Finally, it should be possible to better resolve the velocity structure of the Alpine Fault hanging wall, and compare it to well logs.

Seismic survey layout

Figure 2 shows the survey layout relative to the surface location of the Alpine Fault. Vibe points are green and blue, receiver locations are magenta, red and yellow, and the DFDP-2 surface location is black. Receiver types are summarized in Appendix A, and source types are summarized in Appendix B. Vibe points were repeated many times to accommodate VSP tool moves in the borehole, as well as a 3D rolling patch of 1C and 3C nodal systems (cubes). Two conventional 1C-2D crooked-lines in the approximate dip direction of the Alpine Fault were acquired. This report focuses on initial data results for the longer of the two crooked-lines (green/magenta, west bank of river, Figure 2). Note that the middle ~third of this line is on a valley side above the river that is steeply dipping cross-line to the east, while the ends of the line are on river/glacial sediments. Figure 3 shows the CMP fold after crooked-line binning of Aries receiver line 1 and source line 2.

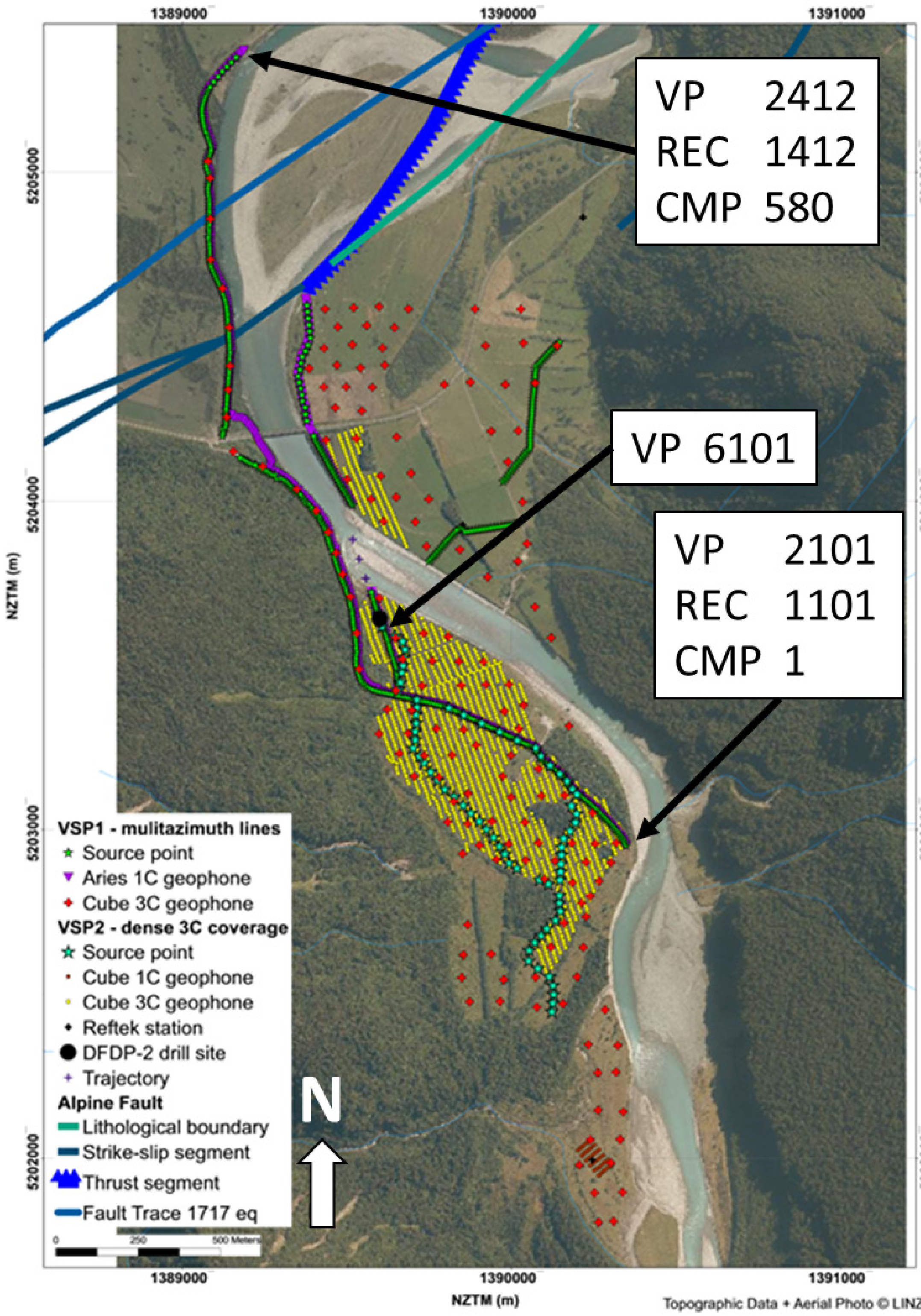

Figure 2. Whataroa valley seismic survey layout. Map courtesy TU Freiberg.

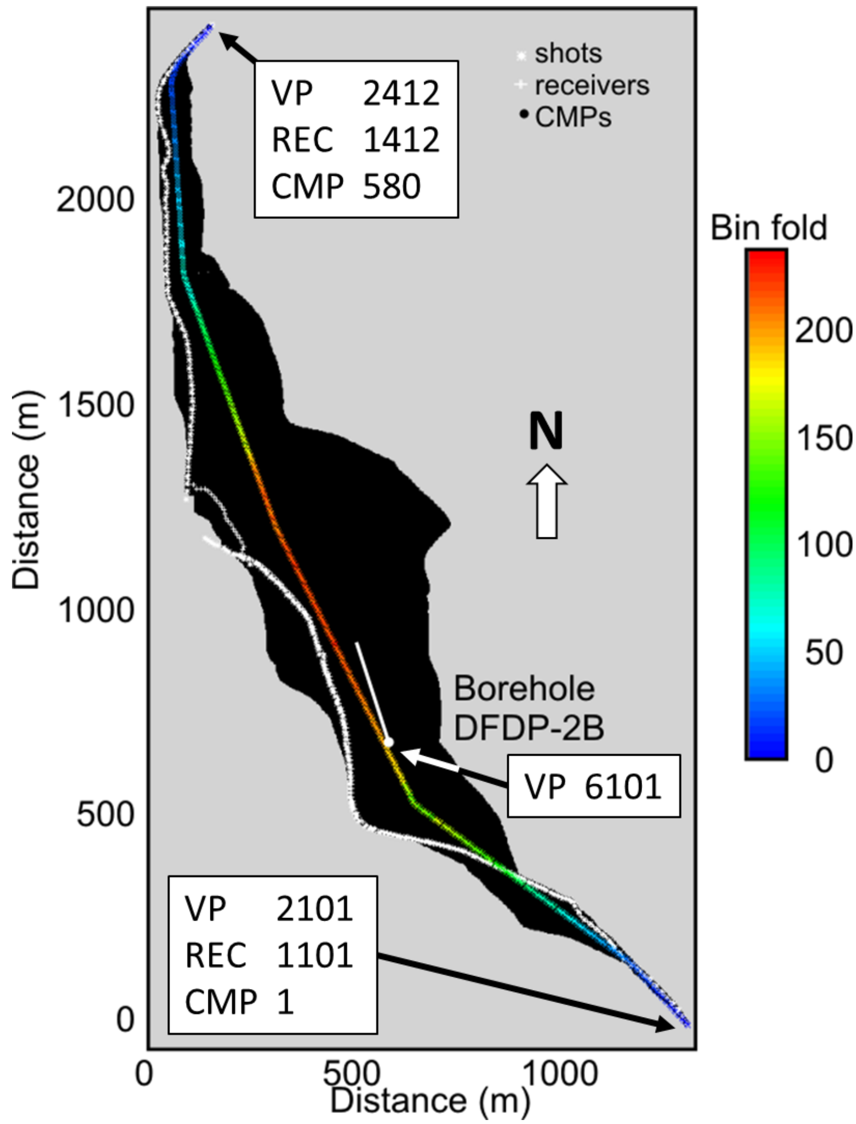

Figure 3. Locations of Aries receiver line 1 and source line 2 (white), DFDP-2 borehole and borehole trajectory (white) CMP locations (black) and the binning line (colour-coded by bin fold). Bins (not shown) are 5x500 m rectangles centered on the binning line.

Zero-offset VSP: Fiber and geophone data comparison

A generalized geologic column based on drillers reports is shown on the left side of Figure 4. The centre of the figure shows strain data from the hDVS system (2 m spatial sampling from surface to 893 m depth) in blue overlain with vertical-component velocity data from the VSP geophone tool in red (1 m spatial sampling from 120 to 400 m depth). Geophone data from 84 to 120 m depth were recorded but are unusable because of casing flexure. A borehole schematic is shown on the right-hand side. Tube waves are visible reflecting off the top of the cement in the well in the geophone data. (Constantinou et al., 2016). A relatively strong refection can be seen from the bottom of one of the casing tubes, below the sediment/schist boundary) with a strong down-going conversion (labeled P and S). It is possible the event labeled P is a casing wave travelling at the velocity of sound in steel, and the event labeled S is actually a P-wave.

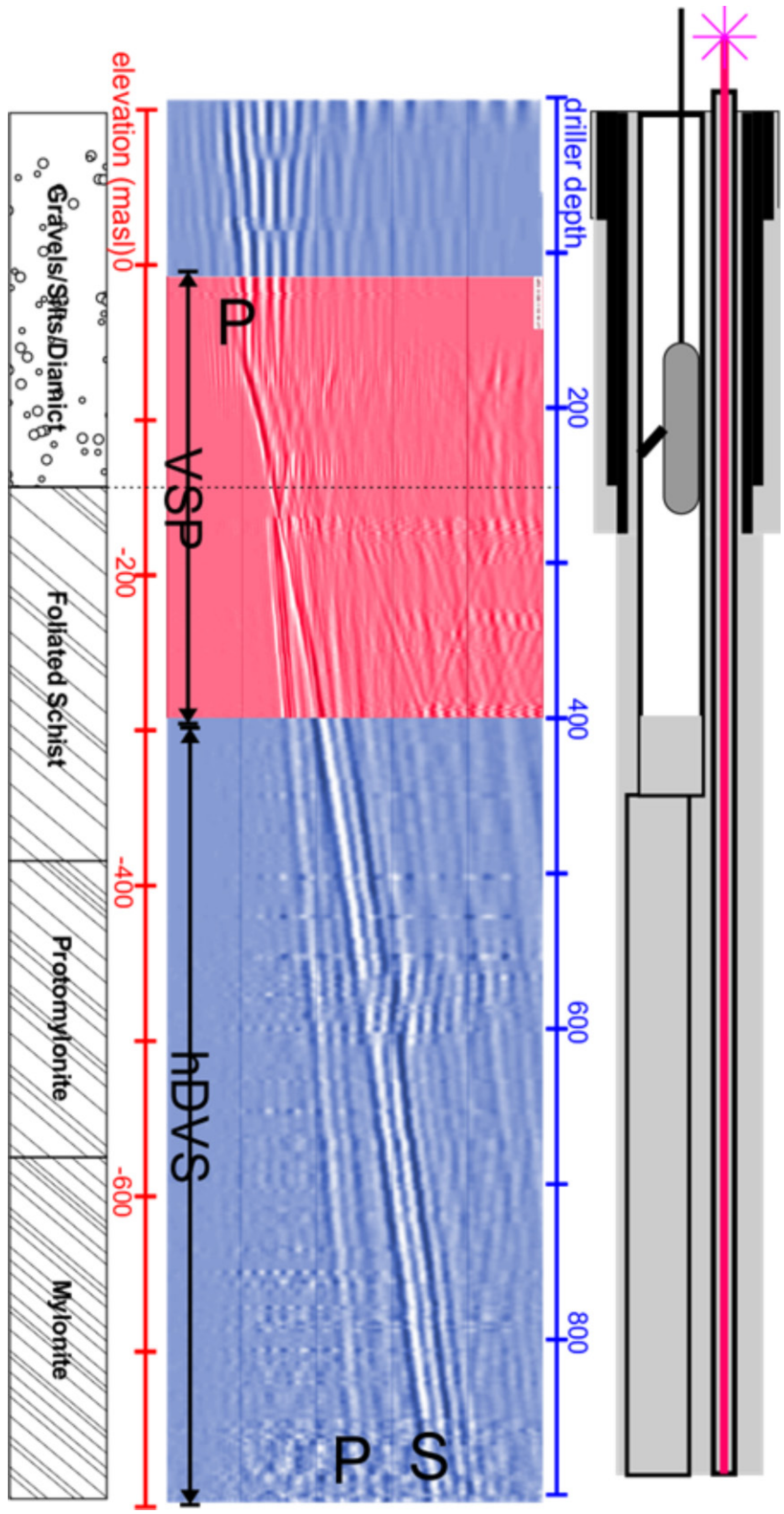

Figure 4. Composite zero-offset VSP plot. VSP vertical component data (velocity) is shown with a red tint from 120-400 m and the DAS output (strain) with blue tint from the surface to 893 m. Tube waves reflecting off the top of the cement in the well are visible in the geophone data (from Constantinou et al., 2016).

Crooked-line: Source gather comparisons

Aries source line 2 was acquired with a vibe point every 10 m along a gravel road, with four sweeps per vibe point. All uncorrelated data were stored on disk. The road services the DFDP-2 well pad as well as a landing area for helicopter tours. We did our best not to sweep when helicopters were flying by, but carried on when there was vehicle traffic on the road. Figure 5a shows Vibe Point 2101 with vehicle noise on a conventional vertical-stack (average) and correlation with the Vibe sweep. Note that noise from the same vehicle has been captured four times at four locations on the road in this gather. The low-frequency noise in the centre of the gather is noise from the flowing river. Figure 5b shows the same data after diversity stacking (weighted-average). The river noise is still present, but the vehicle noise has been suppressed. Figure 6 shows a series of diversity-stacked source gathers progressing from south to north along the line. The direct arrivals and first reflections (top of schist?) are highly asymmetric.

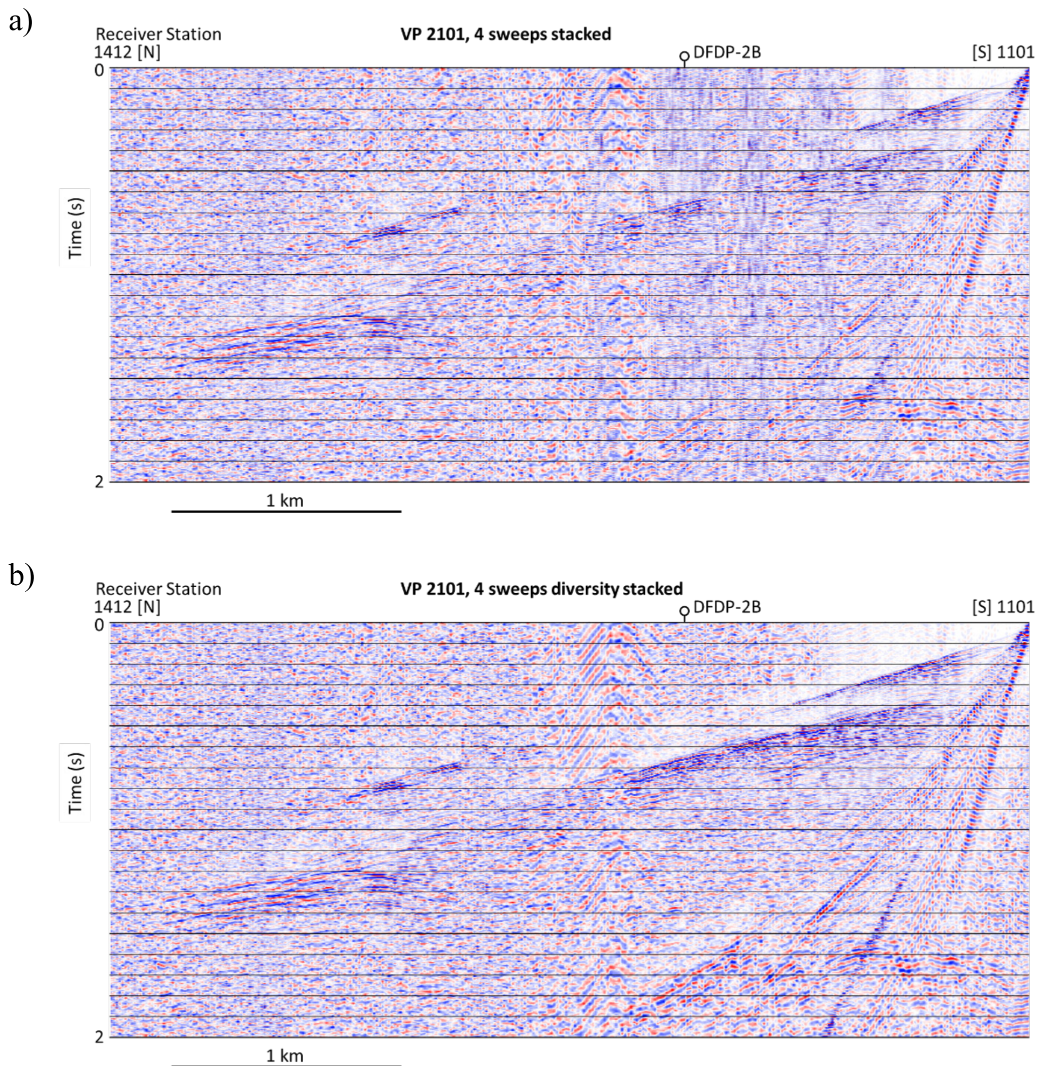

Figure 5. Source gather for VP 2101, with four sweeps stacked and correlated (a) and four sweeps diversity stacked and correlated (b). AGC for display.

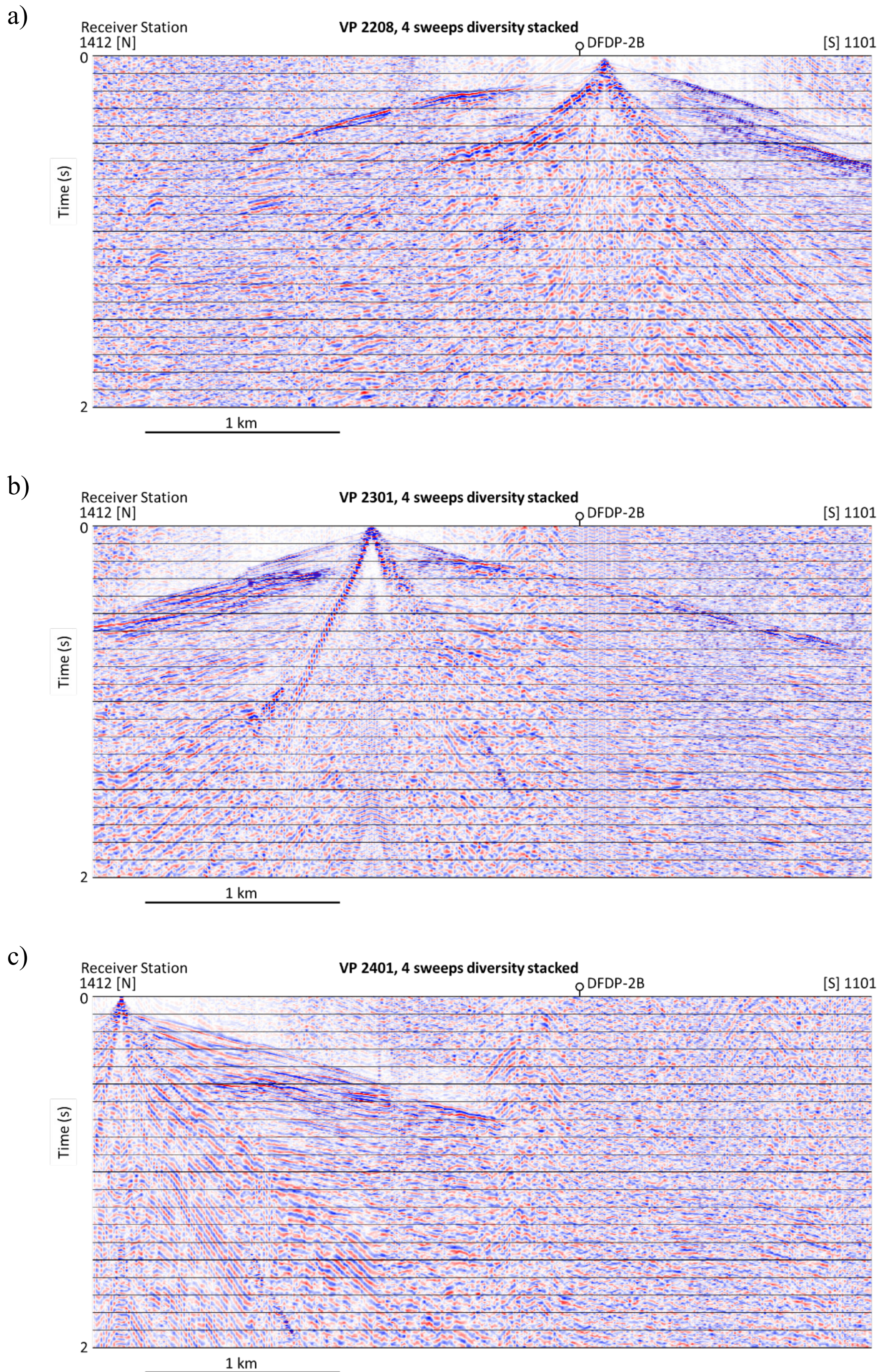

Figure 6. Source gather for VP 2208 (a), 2301 (b) and 2401 (c); four sweeps diversity stacked and correlated. AGC for display.

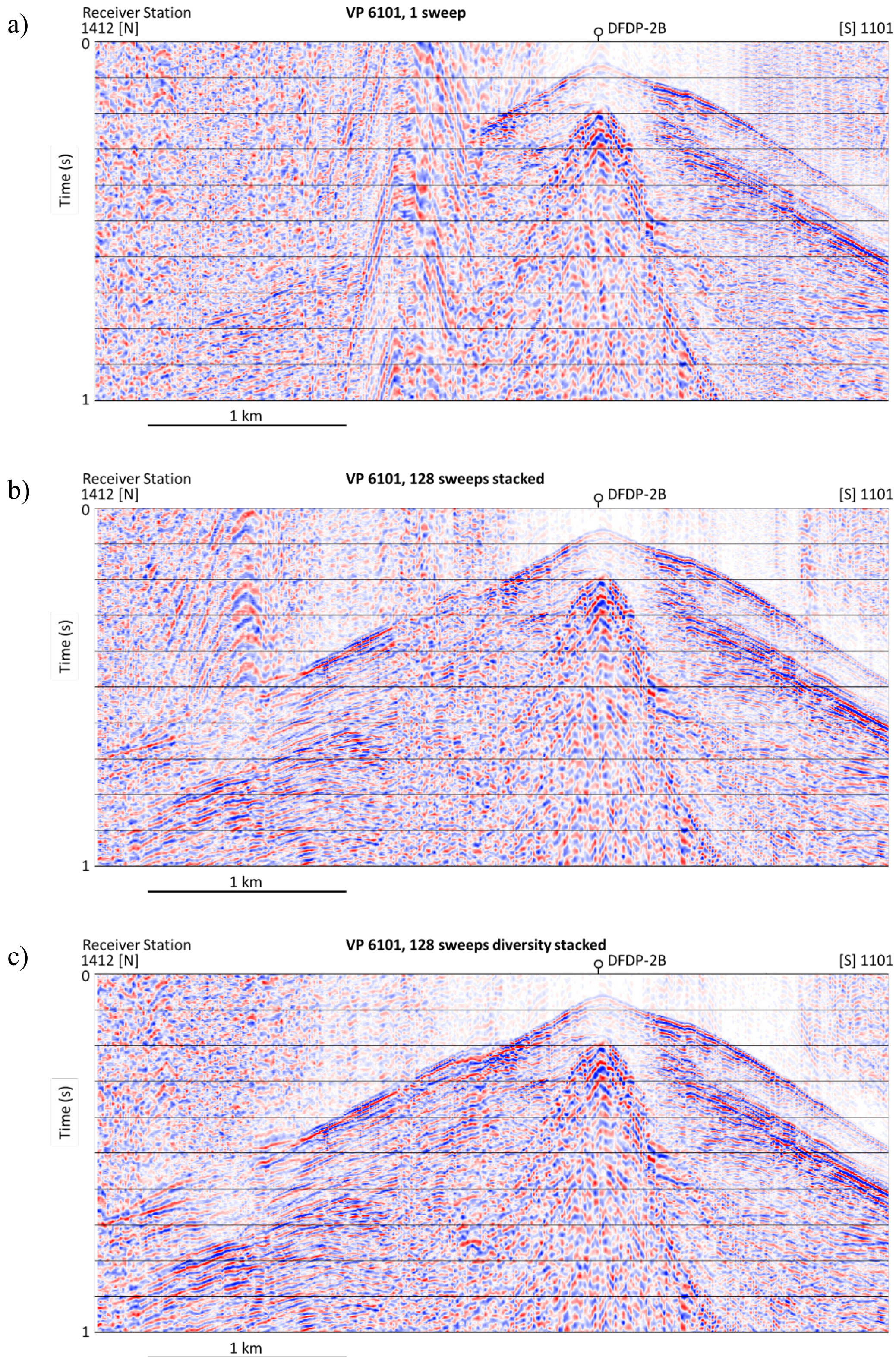

Figure 7. Single sweep (vertical fold=1) from VP 6101, zero-offset VSP (a), conventional stack (vertical fold=128) (b), and diversity stack (vertical fold=128). AGC has been applied for display.

Crooked line: Relationship between number of sweeps and data quality

All uncorrelated shot gathers were stored, which means that while we have a minimum of four sweeps per vibe point, we have up to a maximum of 236 sweeps per vibe point for the zero-offset VSP source point location. If we use all available sweeps for a given vibe point, acquired on different days and with different weather conditions as vibe points were repeated for different VSP tool positions in the well and for different 3D receiver patches, we can significantly improve our data quality. Figure 7 shows a comparison between a single sweep (Figure 7a) and conventional and diversity stacks with 128 vertical fold (Figure 7b and Figure 7c). If we define time gates above and below the direct-arrivals, but excluding the direct arrivals, we can calculate a signal-to-noise ratio for each trace in each source gather. Figure 8 shows a summary of the signal-to-noise mean, median and standard deviation calculated for a variety of vertical folds, for both stacking methods. Interestingly, the signal-to-noise ratio increases for both stacking methods from 2 to 32 sweeps, with the diversity stack being a little bit better than the conventional stack. However, while the signal-to-noise ratio continues to improve as we add sweeps to the diversity stacks, the conventional stacks get worse after 32 sweeps (Figure 8). How many sweeps to use in the field? Generally, we use four sweeps per vibe point, which seems to work well with the high CMP fold generated by our typical 10 m source and receiver spacing. For this study, we used diversity stacks of every sweep available for a given vibe point in the stacked and migrated sections shown below. Note that increased vertical fold has no effect on CMP fold.

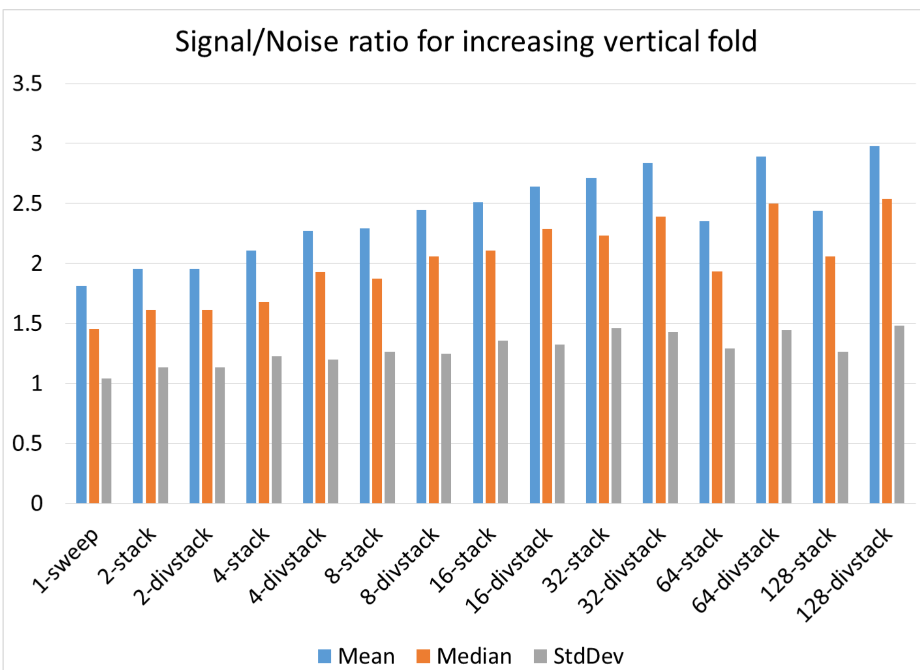

Figure 8. Summary of signal to noise ratios calculated for each trace in conventional and diversity stacked source gathers for 1, 2, 4, 8, 16, 32, 64, and 128 vertical fold.

Crooked line: Common offset gathers

Common offset gathers can be a quick way to determine if the data contain reflections, and if the reflections have any dependence on source-receiver offset and azimuth. Figure 9 shows common offset gathers for +/- 540 m offsets. Both gathers contain events dipping to the south (towards station 1101) as expected for the Alpine fault. Near-surface (0.2-0.5 s) direct arrivals and first reflection (top of schist?) show asymmetry between the positive and negative offset gathers, as expected from inspecting the raw source gathers (Figure 5 and Figure 6).

a)

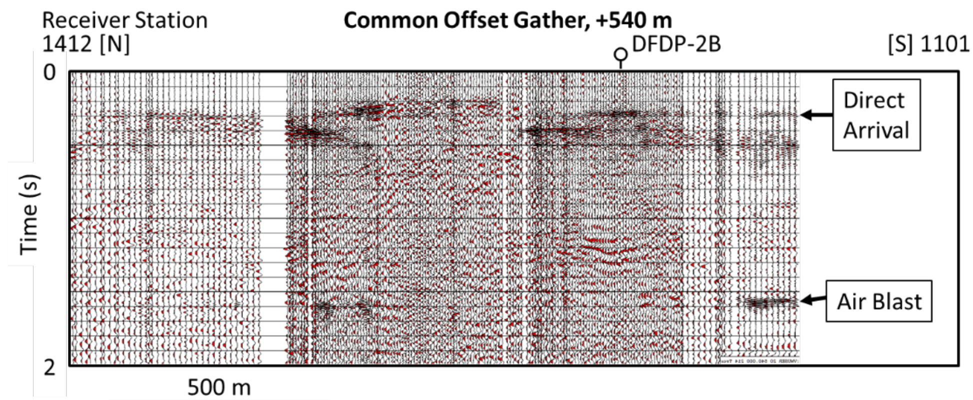

b)

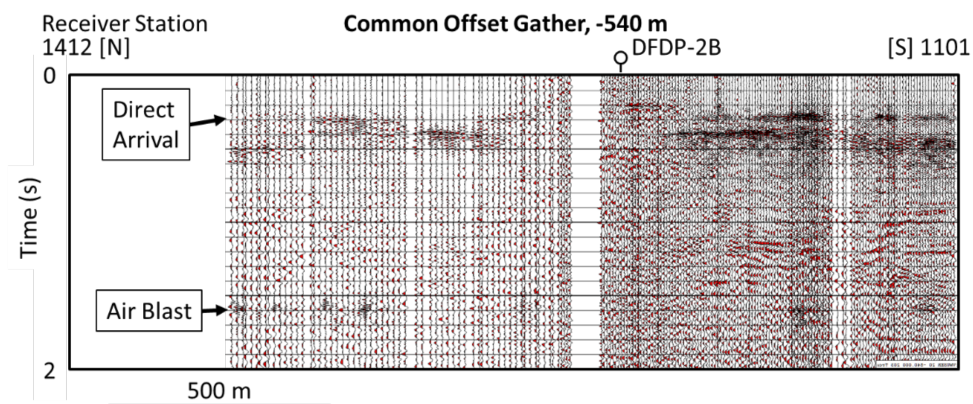

Figure 9. Common offset gathers for source-receiver offsets of +540 m (a) and -540 m (b).

Crooked line: Brute stacks

Figure 10 shows offset limited brute stacks. Gathers have been NMO corrected, but no statics have been applied. A frequency-offset (f-x) deconvolution has been applied to all source gathers pre-stack. In general, events dipping to the south can be interpreted as being related to the Alpine fault. There is very little contribution to these dipping events below about 0.5 s for source-receiver offsets less than 700 m. Figure 11 shows the difference in contributions between positive and negative source-receiver offsets.

a)

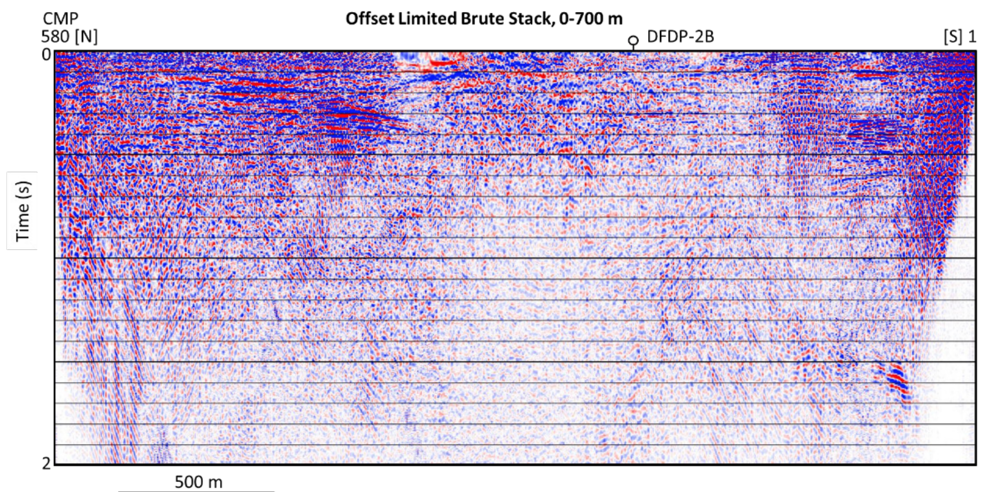

b)

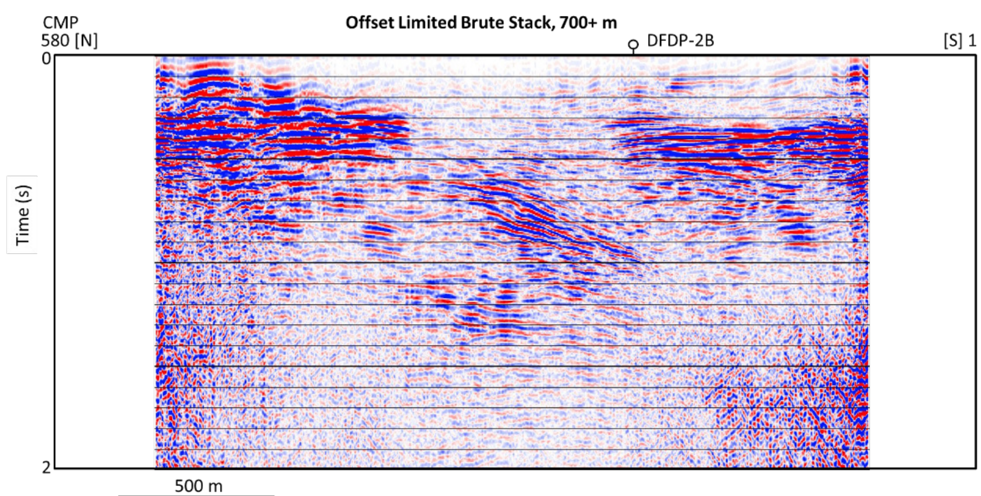

Figure 10. Brute stack with f-x deconvolution applied to gathers before stacking. 0-700 m offsets (a), and 700+ offsets (b). High gain for display, no AGC.

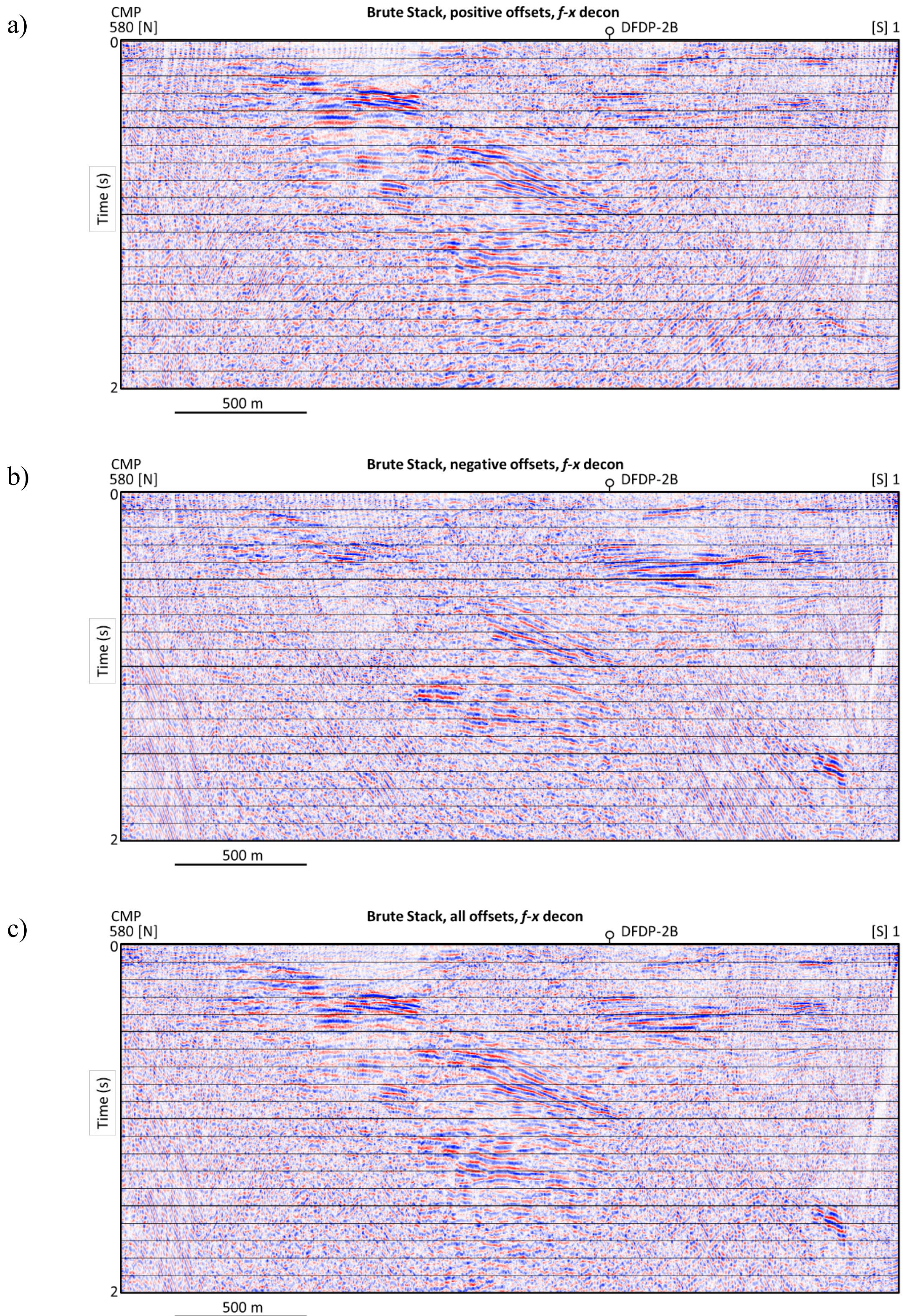

Figure 11. Brute stack with f-x deconvolution applied to gathers before stacking. Positive source-receiver offsets (a), Negative source-receiver offsets (b) and all source-receiver offsets (c). AGC for display.

Crooked line: Migrated stack

We tried to process the Whataroa line to achieve an interpretable migration section. There is a lot of noise in the data and probably some sideswipe. We applied standard processing, which included true amplitude recovery, air blast attenuation, radial filtering, and Gabor deconvolution. Refraction statics were calculated from the first break picks and applied using a final datum of 100 m with a replacement velocity of 2350 m/s. Figure 12 shows the first source gather before and after processing, and the elevation profile along the line. We see irregularities in the first breaks caused by lateral velocity changes and out-of-plane events. Event A arrives earlier than direct arrivals with much shorter offsets. Event B is noise we interpret to be caused by the river water crashing against the riverbanks. Events C and D are of the kind seen in areas of structural complexity, and could be fault-related. We stacked the line using crooked line binning. Figure 3 shows the shot and receiver locations and the location of the binned line with its fold. After stacking the data, we migrated the section using post-stack finite difference time migration. The stacked and migrated sections are shown on Figure 13. There is a lot of noise in the stacked section below 1.5 s so the data do not migrate well here.

Crooked line: Interpretation

To interpret the data and tie it to borehole information, we converted the time migrated section to depth using the velocities obtained from the VSP data (Schlumberger Internal Report) for the top 800 m and velocities from data processing below that depth. Figure 15 shows this depth-converted section with the location of the deviated borehole DFDP-2B and our interpretation. We interpreted the location of the Alpine Fault from the observed contrasting dips of reflections. The depth of the Alpine Fault matches well the depths documented in published work (Norris et al., 2012) for the Whataroa area. The deviated DFDP-2B borehole reached a depth of 893 m (724 m TVD) and terminated in mylonitic rocks which are inferred to be within 200–300 m of the principal slip zone (Townend et al., 2016). The location of our interpreted Alpine Fault fits this scenario.

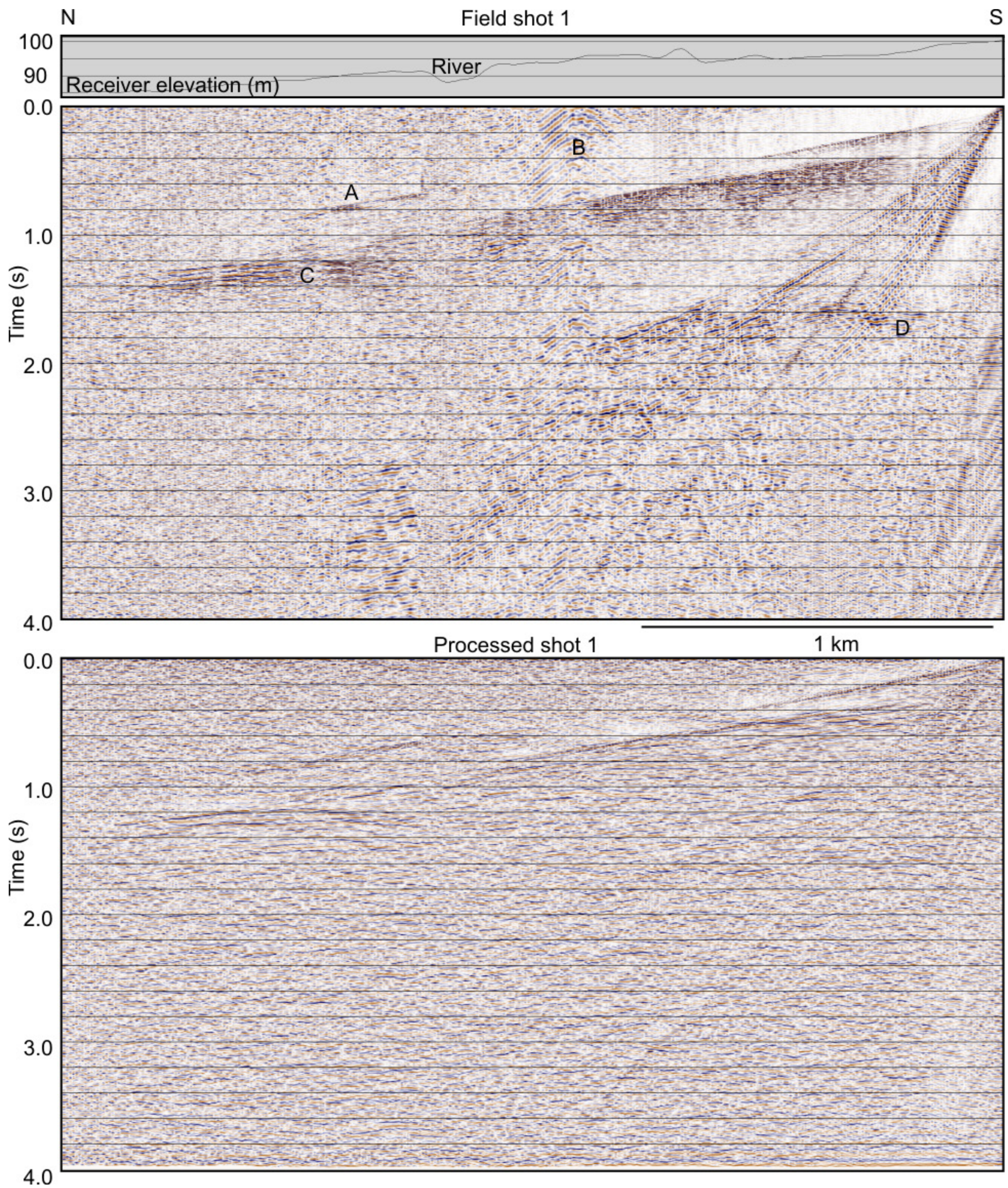

Figure 12. The first source gather (VP 2101) from the reflection seismic survey at Whataroa (cf. Figure 5).

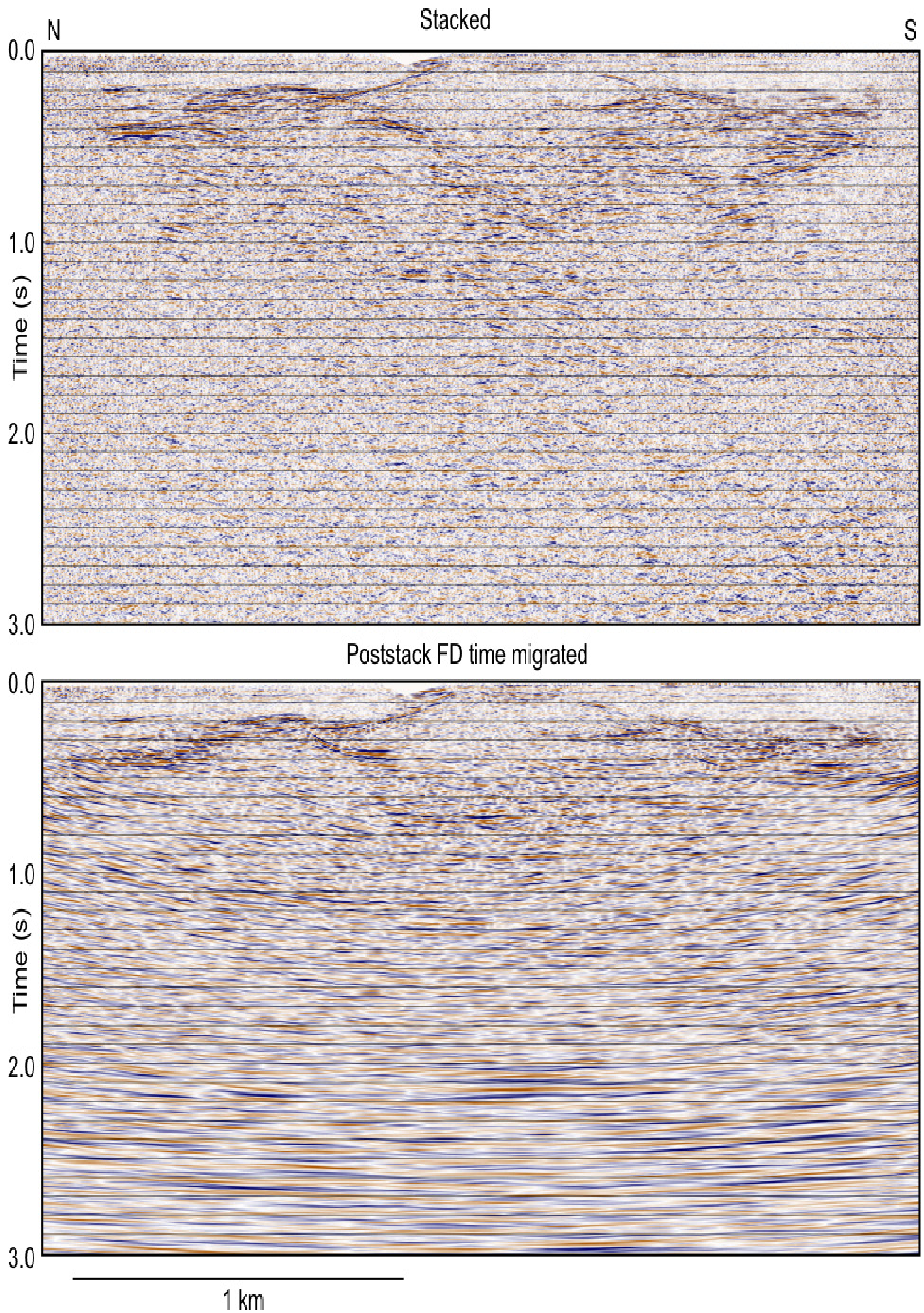

Figure 13. The stacked and poststack time migrated section.

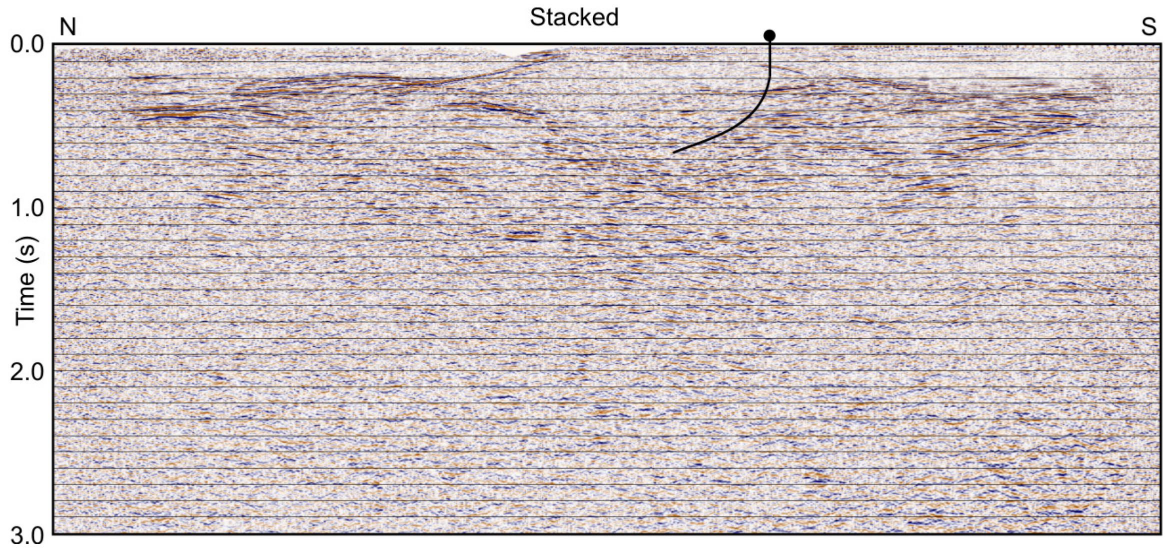

Figure 14. The top 3 s of the crooked-line section with the location of the DFDP-2B borehole. The borehole trajectory has been converted to time using velocities from the zero-offset VSP.

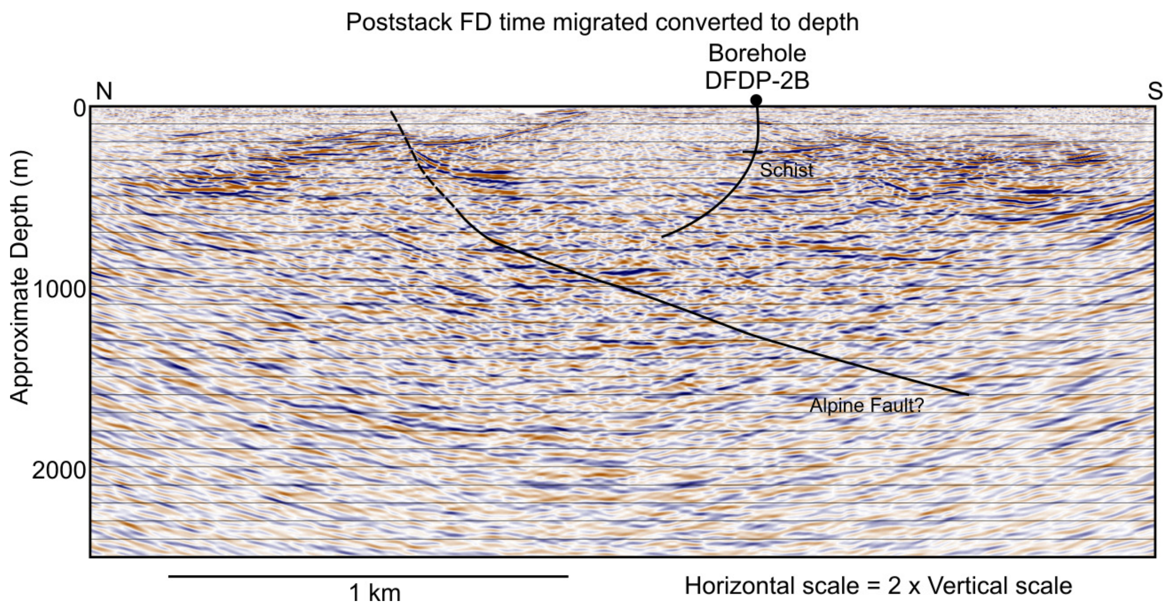

Figure 15. The top 2500 m of the depth-converted poststack time migrated section with the location of the DFDP-2B borehole and our interpretation of the Alpine Fault.

HAURAKI RIFT (FIRTH OF THAMES)

Geology overview

Geological and geophysical studies of the Hauraki Rift (Schofield, 1967; Hochstein and Nixon, 1979; Edbrooke, 2001; Haywood and Grenfell, 2010) show it to be part of an active continental rift structure which started to form after the collision of the Indian and the Pacific plates. Although poorly orientated to accommodate back-arc extension associated with New Zealand's subduction margin, normal faults bounding the rift lie parallel to basement terrane boundaries (Edbrooke, 2001). The rift is bounded on the east by the Hauraki Fault, a major normal fault which dips about 70±10° to the west and has a throw of 3-5 km. In the southern part of the rift, the Kerehepi Fault, which dips at 70-80° to the west and is considered to be active (Houghton and Cuthbertson, 1989), controls the major central basement uplift. Transverse faults crossing the rift cause up to 3 km horizontal offsets of the major normal faults.

The southern part of the Hauraki Rift is filled with about 3 km of Quaternary and Neogene sediments and is bounded on the western side by Jurassic metagreywackes. In the near surface the thin water-saturated low velocity layer is underlain on each side of the Piako River by up to 500 m of Quaternary sediments having a velocity of 1520-1570 m/s. The velocities of the deeper Neogene rocks are 2200-3000 m/s, and the velocity of 3770 m/s measured in the central uplift is typical of shallow greywackes observed elsewhere in New Zealand. Refraction seismic data showed the average velocity of the basement rocks to be 3450 m/s (Hochstein and Nixon, 1979).

The Kerepehi Fault is only well delimited at the surface as far north as Ngatea (Persaud et al., 2016), although gravity modelling indicates continuity of the deeper structure to the north (Hochstein and Nixon, 1979). Recent active fault mapping and analysis of tilting of geomorphic surfaces also suggests that the Kerepehi fault extends up to the coast under younger undeformed alluvial and coastal sediments (Persaud et al., 2016).

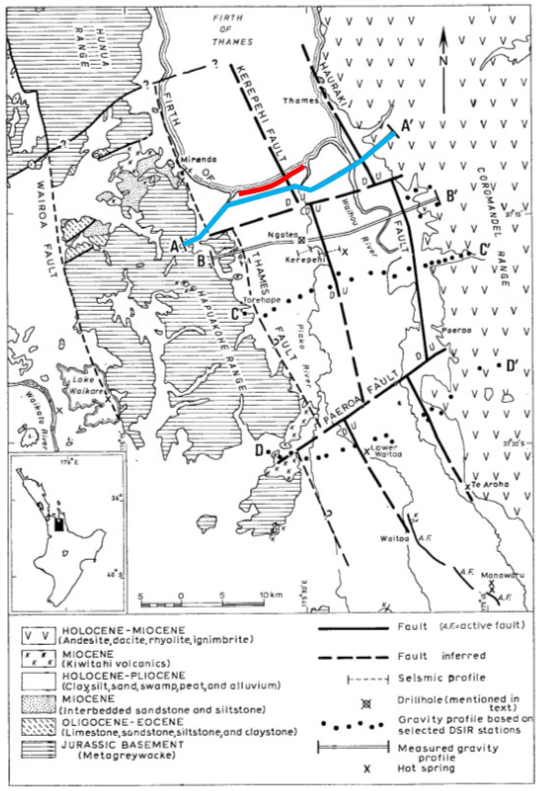

Figure 16. Location of seismic line within the Hauraki rift (red) and gravity profile A-A' (blue) (from Hochstein and Nixon, 1979).

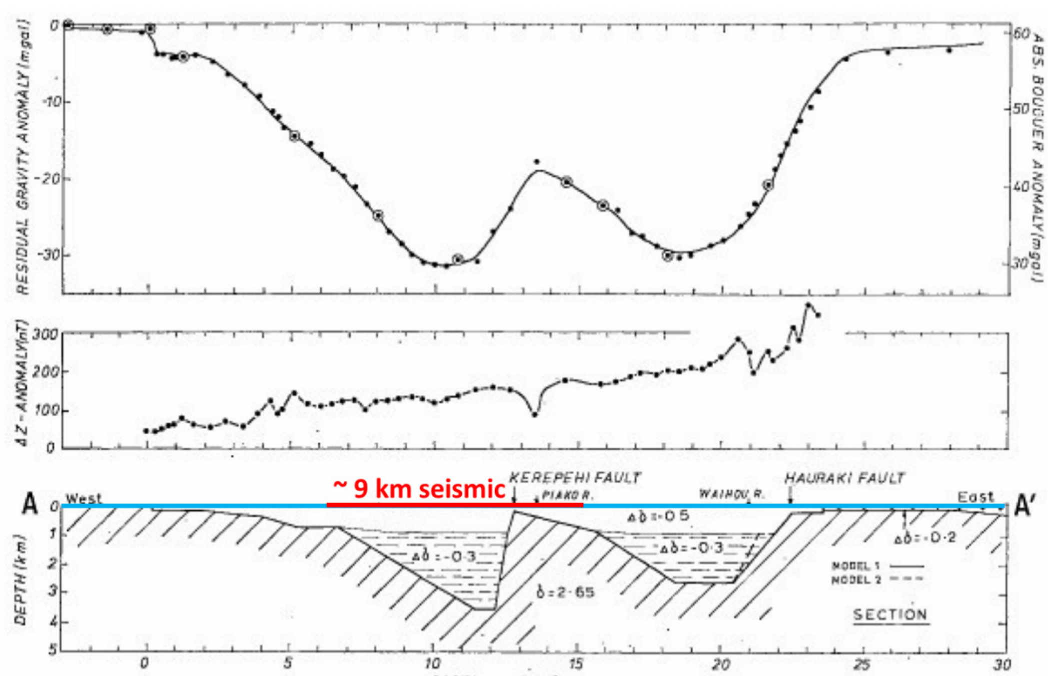

Figure 17. Observed and computed Bouguer gravity anomalies (top), observed magnetic anomalies (middle), and approximate location of 2016 seismic line on A-A' gravity model (bottom) (from Hochstein and Nixon, 1979).

Purpose of seismic work

The Hauraki Rift is a poorly understood ~30 km wide onshore-offshore extensional structure located 30 km to the east of the Auckland and Hamilton metropolitan areas (Hochstein et al., 1986). It is over 220 km in length extending from the Taupo Volcanic Zone (SSE) to potentially offshore Whangarei (NNW); (Hochstein and Nixon, 1979; Hochstein et. al., 1986), and contains the known active Kerepehi Fault. Individual 20+ km long fault segments mapped to date are thought to produce >M6-7 events, each segment with a recurrence interval of 2500-9000 years (de Lange and Lowe, 1990; Chick et al, 2001; Persaud et al., 2016). This tectonic feature is deemed to represent the primary seismic risk to the Auckland and Waikato regions (Hull et al., 1995; Wright et al., 2009).

Line 1 investigates the lesser known northern Kerepehi Fault segment as modelled by Hochstein and Nixon (1979; Figure 16 and Figure 17) and interpreted as active by Chick et al. (2001), allowing the northward trend of activity to be determined. It also links gravity modelling and the near seafloor sediment discontinuities, interpreted offshore by Chick (1999) from near seafloor data as faults, with a more detailed view of the deeper structure. Figure 16 shows the location of the seismic line in the Hauraki Rift overlain on a geology map, where the red line shows the seismic line location and the blue line highlights the location of gravity profile A-A’ shown in Figure 17 (Hochstein and Nixon, 1979).

Seismic survey layout

The Hauraki Rift 1C-2D crooked-line was conducted on top of a stop-bank between the Firth of Thames (North) and farmland (South; Figure 18). Receivers were single-component SM-24 marsh phones at a 10 m spacing. Vibe points were also every 10 m. As the line is about nine kilometers long and we have a maximum of six kilometers of equipment, the survey was conducted as a rolling spread. The top of the stop-bank is very flat. GPS elevations do not vary by more than 10 cm, which may well be within GPS error.

Figure 18. Hauraki Rift seismic survey layout.

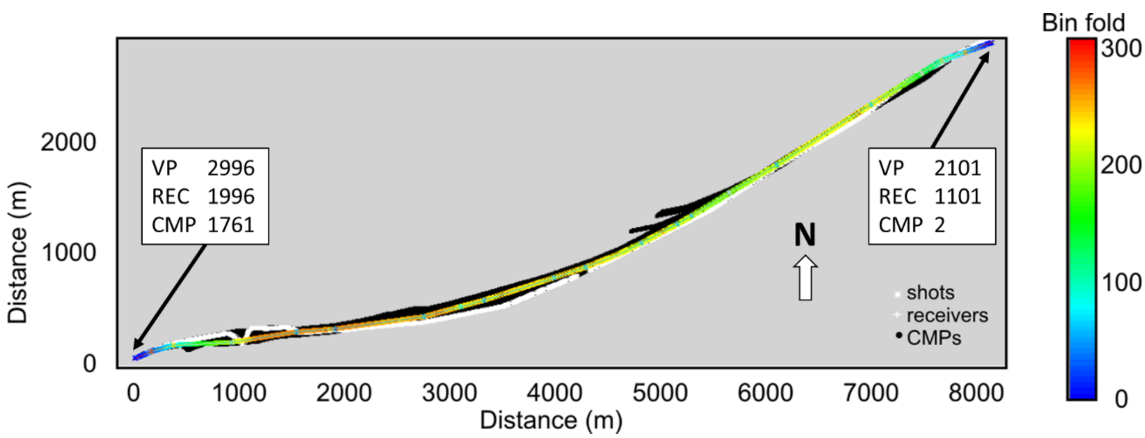

Figure 19. Locations of Aries receiver line 1 and source line 2 (white), CMP locations (black) and the binning line (colour-coded by bin fold). Bins (not shown) are 5x220 m rectangles centered on the binning line.

Crooked-line: Earthquake

Figure 20 shows sequential uncorrelated source gathers acquired before (a) and during (b) arrivals from a M5.2 earthquake that occurred at a depth of 54 km on the South Island. Most of the earthquake energy is below 10 Hz. As such it is attenuated by the geophone hardware when recorded, and is removed when the gathers are correlated with the Vibe sweep.

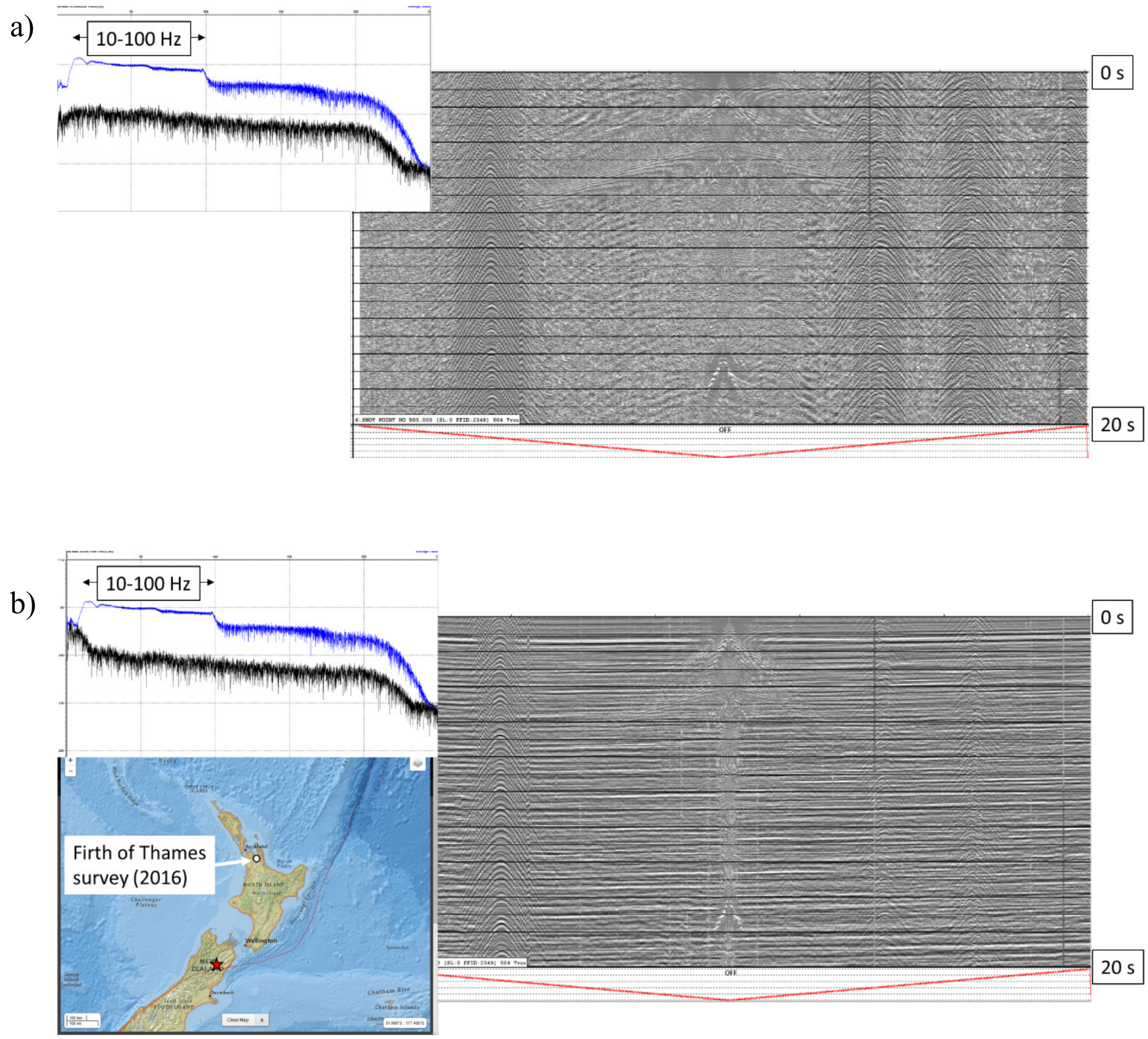

Figure 20. Source gather (FFID 2348) acquired before (a) and during (FFID 2349) arrivals from a M5.2 earthquake (a). Earthquake location is shown as a red star on inset map (USGS, 2016).

Crooked line: Processing

We processed the Hauraki line to attenuate noise and enhance signal. We applied true amplitude recovery, air blast attenuation, predictive deconvolution, and Gabor deconvolution. Figure 21 shows field source gathers (left) and the same gathers after processing (right). Surprisingly, given how flat the region is, the gathers show irregularities in the first breaks caused by lateral velocity changes and out-of-plane events.

Refraction statics were calculated from the first break picks and applied using a final elevation datum of 37 m with a replacement velocity of 1000 m/s. Figure 22 shows the refraction velocity model. The velocities mapped here agree with those of Hochstein and Nixon (1979), who calculated velocities of 500-800 m/s for the low velocity layer, and 1520-1570 m/s for the underlying Quaternary sediments.

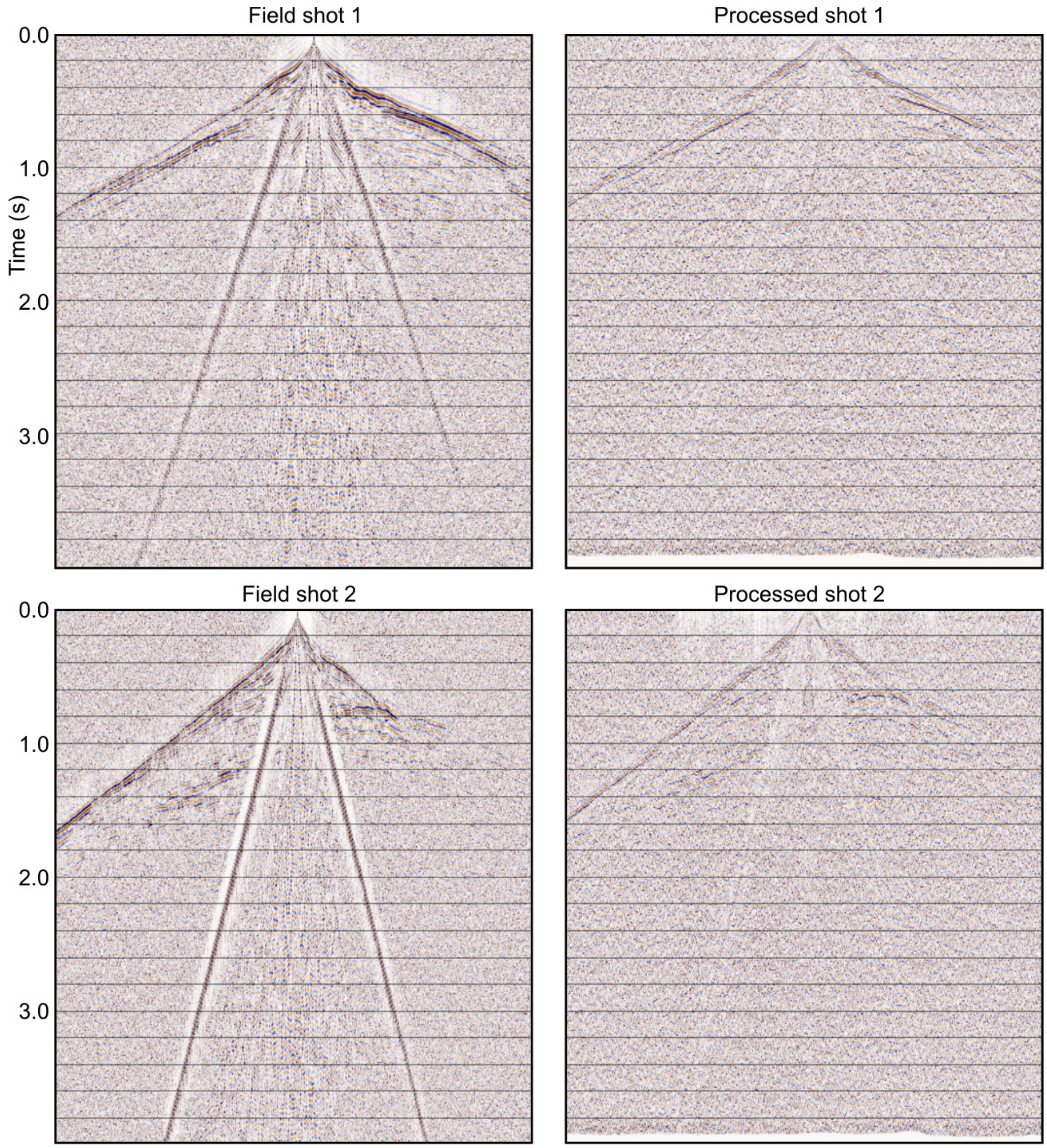

Figure 21. Examples of shot gathers. On the left are field shots showing air blast noise and interesting first breaks. On the right are the same gathers after processing.

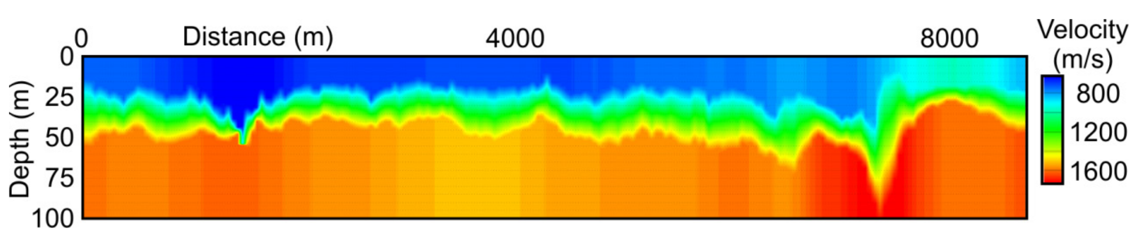

Figure 22. The near-surface velocity model obtained from refraction statics analysis.

We stacked the line using crooked line binning and migrated the data using post-stack finite difference time migration, prestack Kirchhoff time migration and prestack Kirchhoff depth migration. These three migrations are shown in Figure 23. It is interesting to observe the differences between the images. To the west of the uplift on the right the prestack data appear faded out and the poststack data appear to be imaged better. The prestack depth migrated section has imaged the basement reflectors poorly. This could be due to the use of incorrect velocities, as the velocities were hard to establish.

Crooked line: Interpretation

Figure 24 shows the seismic line with our interpretation of the major structural features annotated. The central basement ridge and Kerehepi Fault are seen clearly in the east. The top of the basement, although not well imaged, can be seen to dip from west to east. In the centre of the line are reflectors representing the Neogene sedimentary graben fill, which are tilted to the east and appear to be wedge shaped, with the thick end of the wedge to the east. This implies the sediments have been deposited while the Kerepehi fault was active (growth fault).

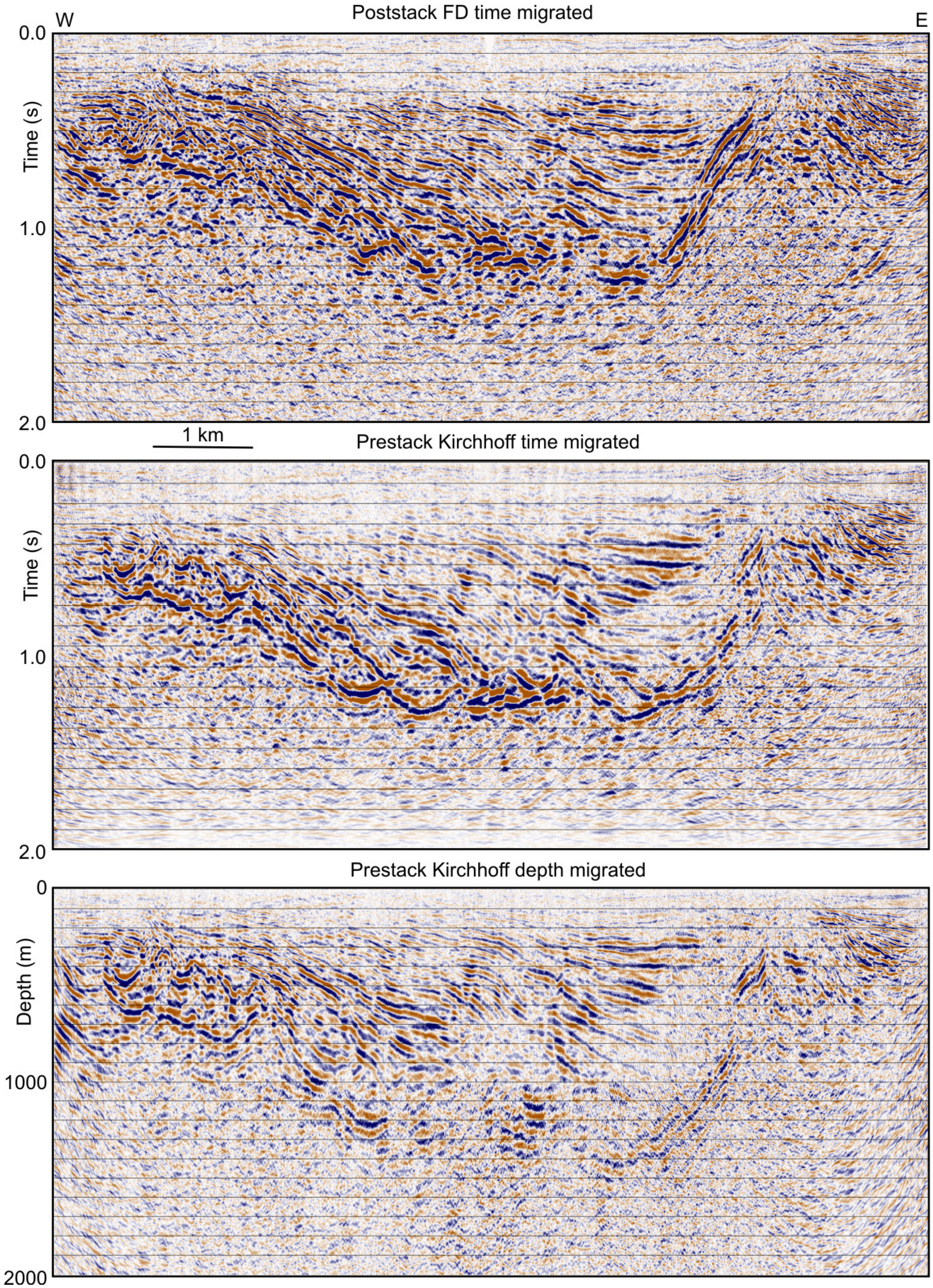

Figure 23. Poststack migrated, prestack time migrated and prestack depth migrated versions of the line.

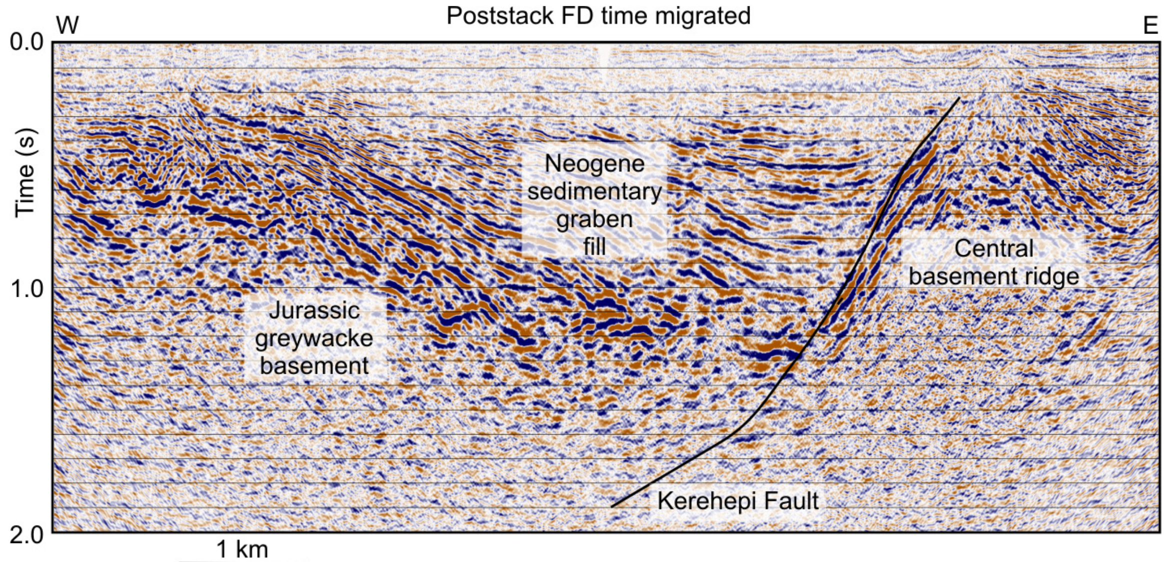

Figure 24. Our interpretation of the Hauraki line with the main structural features annotated. (Compare with Figure 17).

DISCUSSION AND FUTURE WORK

Good initial results were obtained for the zero-offset VSP in borehole DFDP-2b. There is a good match between the vertical component geophone data (velocity) and the DAS data (strain). These data need to be processed to a corridor stack and utilized directly in the surface seismic data interpretation. The horizontal channels also need to be processed and interpreted. The multi-offset VSP geophone and DAS data should be processed, matched to the surface seismic, and interpreted. A short 1C surface seismic line that is roughly located above the borehole trajectory has not yet been processed. The cube and seismometer data also need to be considered. We obtained fairly good images of the base of sediments and, we believe, of the Alpine Fault. Further processing to see if clearer images can be obtained should be conducted. The stacked and migrated sections shown in this report can be interpreted in greater detail.

The North Island survey has produced decent images of structure within the Hauraki Rift, particularly of the base of sediments and of sediments deposited in the hanging wall of the active Kerepehi fault. These data may also benefit from further processing, and certainly require a more detailed interpretation and integration with other geophysical data available in the area.

ACKNOWLEDGEMENTS

DFDP-2 was principally funded by the International Continental Drilling Project, the Marsden Fund of the Royal Society of New Zealand, the Ministry of Business, Innovation, and Employment, GNS Science, Victoria University of Wellington and the University of Otago. This experiment was funded by the Earthquake Commission and Victoria University of Wellington, and grants held by the University of Calgary, University of Alberta and TU Freiberg.

The authors would also like to thank Halliburton (SeisSpace) and Schlumberger (Vista) for the use of software donated to the University of Calgary. We also thank Rupert Sutherland of the Victoria University of Wellington for comments and suggestions about figures contained in this report.

REFERENCES

Chick, L. M., 1999, Potential tsunami hazard associated with the Kerepehi Fault, Hauraki Gulf, New Zealand, MSc thesis, The University of Waikato.

Chick, L.M., de Lange, W.P., and Healy, T.R., 2001, Potential tsunami hazard associated with the Kerepehi Fault, Firth of Thames, New Zealand: Natural Hazards, **24**, 309-318.

Constantinou, A., Schmitt, D., Kofman, R., Kellet, R., Eccles, J., Lawton, D., Bertram, B., Hall, K., Townend, J., Savage, M., Buske, S., Lay, V., and Gorman, A., 2016, Comparison of fiber-optic sensor and borehole seismometer VSP surveys in a scientific borehole: DFDP-2b, Alpine Fault, New Zealand: SEG Internat. Expo. and 86th Ann. Mtg., Dallas, Soc. Expl. Geophys., Expanded Abstracts, 5608-5612.

Edbrooke, S. W. 2001, Geology of the Auckland Area, 1:250,000 geological map 3, Institute of Geological and Nuclear Sciences, Lower Hutt, New Zealand

GNS Science Public Wiki: https://wiki.gns.cri.nz/DFDP/DFDP-2_Whataroa_River/DFDP-2_FAQs, accessed October 25, 2016.

Google Earth, 2016, Google Earth version 7.1.7.2600 software downloaded and installed from http://www.google.com/earth/index.html, images accessed March 18, 2016.

Hall, K.W., Bertram, K.L., Bertram, M.B., and Lawton, D.C., 2011, New Zealand acquisition, spring 2011, CREWES Research Report, 38, **23**, 1-32.

Haywood, B. W. and H. R. Grenfell, 2010, The Puketoka Formation and the age of the Hauraki Graben. Preconference field trip, Auckland: Geoscience Society of New Zealand Miscellaneous Publication 129B, 7pp.

Hochstein, M. P. and I. M. Nixon, 1979, Geophysical study of the Hauraki Depression, North Island, New Zealand, New Zealand Journal of Geology and Geophysics, 22:1, 1-19, DOI: 10.1080/00288306.1979.10422550.

Hochstein, M. P., Tearney, K., Rawson, S., Davey, F.J., Davidge, S., Henrys, S., and Backshall, D., 1986, Structure of the Hauraki Rift (New Zealand), *in* Recent crustal movements of the Pacific region, edited by Reilly, W.I., and Hurford, B.E.: Bulletin - Royal Society of New Zealand, **24**, 333-348.

Houghton, B. F. and Cuthbertson, A.S., 1989, Kaimai, Geological Map of New Zealand 1:50000, T14BD, 35. Department of Scientific and Industrial Research, wellington, New Zealand.

Hull, A., Mansergh, G., Townsend, T. and Stagpoole, V., 1995, Earthquake hazards in the Auckland region. Prepared for the Auckland Regional Council. Auckland Regional Council Technical Publication 57.

de Lange, P. J. and Lowe, D.J., 1990, History of vertical displacement of Kerepehi Fault at Kopouatai Bog, Hauraki Lowlands, New Zealand, since c. 10,700 years ago: New Zealand Journal of Geology and Geophysics, **33**, 277-283.

Lawton, D.C., Bertram, M.B., Hall, K.W., Bertram, K.L, Pettinga, J., 2011, Post-earthquake seismic reflection survey, Christchurch, New Zealand, CREWES Research Report, 66, **23**, 1-16.

Lawton, D.C., Bertram, M.B., Hall, K.W., Bertram, K.L., Pettinga, J., 2012, Post-earthquake seismic reflection survey, Christchurch, New Zealand: SEG 82nd Ann. Mtg., Las Vegas, Soc. Expl. Geophys., Expanded Abstracts, 1-5.

Lawton, D.C., Bertram, M.B., Hall, K.W., Bertram, K.L., Pettinga, J., 2013, Imaging Unknown Faults in Christchurch, New Zealand, after a M6.2 Earthquake, 75th EAGE Conference & Exhibition incorporating SPE EUROPEC 2013 London, UK, 10-13 June 2013, 1-5.

Norris, R. J., A. F. Cooper, V. Toy, S. Read and L. Easterbrook, 2012, Three-dimensional structure of the Alpine Fault in the region around the Waiangi-taona and Whataroa Rivers, University of Otago, Department of Geology,

Persaud, M., Villamor, P., Berryman, K. R., Ries, W., Cousins, J. Litchfield, N. and Alloway, B. V., 2016, The Kerepehi Fault, Hauraki Rift, North Island, New Zealand: active fault characterisation and hazard: New Zealand Journal of Geology and Geophysics, **59**, 117-135.

Schofield, J. C., 1967, Sheet 3 Auckland. Geological Map of New Zealand 1:250 000. New Zealand Department of Scientific and Industrial Research, Wellington.

Sutherland R., Townend J., Toy, V., and the DFDP2 Team, 2015, DFDP-2 completion report. GNS Science Report SR2015/50

Townend, J., Eccles, J., Kellet, R., Buske, S., Constantinou, A., Schmitt, D., Bertram, M., Hall, K., Savage, M., Gorman, A., Kofman, R., Benson, A., Lay, V., Gulley, A., McNab, A., Lindsay, D., Hopp, C., Mann, C., Bodenburg, S.B., Kleine, F., Lepine, P., Bowman, H., Broderick, N., Capova, L., Lawton, D., 2016, Seismic Experiment Acquisition Report: GNS Science Report, 2016/36.

USGS, 2016, http://earthquake.usgs.gov/earthquakes/eventpage/us20004ywf#general_region, accessed March, 2016.

Wright, K., Baldi, M., Van Dissen, V., Salinger, J., Dellow, G., Page, M., Power, W., King, D., and Lindsay, J., 2009, Natural hazards and their impacts: Auckland region. Prepared for the Auckland Regional Council. Auckland Regional Council Technical Publication 2009/2010.

APPENDIX A

Table A.1. Recording systems and receiver types deployed in the field for the Whataroa Valley (Alpine Fault) seismic survey.

	Recorder	Number of receivers	Spatial sampling (m)	Time sampling (ms)	Coupling	#C	Receiver type	Field Picture
Borehole	Schlumberger hDVS	N/A	2	1.0	Cemented	1C	Fiber-optic cable; 3x single mode, 3x multi-mode	
Borehole	Sercel Slimwave	4	1	0.5	Clamped	3C	OMNI 2400 15 Hz geophones, 4 sondes 15 m apart	
Borehole	IESE	4	Sparse	5.0	Nearby monitor wells, 29 m deep.	3C	Short-period HS-1-LT 4.5 Hz seismometer	
Surface	Inova (ARAM) ARIES SPMLite	600	10	1.0	Spike	1C	Inova SM-24 10 Hz geophones	
Surface	Omnirecs Data Cube 3	160	10	2.5	Spike	3C	Oyo-Geospace 4.5 Hz geophones	
Surface	DSS Cube	40	10	1.25	Spike	1C	Oyo-Geospace 4.5 Hz geophones	
Surface	Reftek 130	5	Sparse	2.0	Buried 0.5m	3C	Geospace HS1-3C 2 Hz seismometers	

APPENDIX B

Table B.1. Vibroseis sweep parameters

Parameter	Sweep 1	Sweep 2	Sweep 3	Sweep 4
Survey	Whataroa Zero-offset	Whataroa Multi-offset and 2D survey	Whataroa Far-offset hDVS	Firth of Thames 2D survey
Sweep Length	16 s	16 s	16 s	16
Low Frequency	10 Hz	10 Hz	10 Hz	10 Hz
High Frequency	200 Hz	150 Hz	60 Hz	100 Hz
Type	Linear	Linear	Linear	Linear
Taper	100 ms cosine	100 ms cosine	100 ms cosine	100 ms cosines
Listen Time	4 s	4 s	10 s	4 s
Number of sweeps	2	4	20–50	4

a)

b)

Figure B.1. University of Calgary IVI Envirovibe (a) and University of Otago weight-drop trailer (b).